C. Wilson
Department of Marine Engineering,
Dalian Maritime University,
Dalian 116026, PR China

B. Borgmeyer

R. A. Winholtz

H. B. Ma[1]
e-mail: mah@missouri.edu

Department of Mechanical and Aerospace Engineering,
University of Missouri–Columbia,
Columbia, MO 65201

D. Jacobson

D. Hussey

National Institute of Standards and Technologies,
100 Bureau Drive,
Gaithersburg, MD 20899

Thermal and Visual Observation of Water and Acetone Oscillating Heat Pipes

A visual and thermal experimental investigation of four oscillating heat pipes (OHPs) was conducted to observe fluid flow of liquid plugs and vapor bubbles in the OHP and its effect on the temperature distribution and heat transfer performance in an OHP. These four OHPs consist of an open loop water OHP, an open loop acetone OHP, a closed loop water OHP, and a closed loop acetone OHP. These copper OHPs were constructed identically with all six turns in the same plane. They were constructed out of 1.65 mm inner diameter copper tubing and copper heat spreading plates in the evaporator and condenser regions. The heat pipes were charged at a filling ratio of about 50%. The results show that the acetone OHP at low power performs better than the water OHP, while at high power the water OHP exceeds the acetone OHP. The experimental results show that both the acetone and water closed loop OHPs had reduced movement in the connecting turn between the two sides. However, in the water closed loop OHP, this prevented circulation altogether. Comparing the water closed loop OHP to the water open loop OHP, their flow patterns were similar. Therefore, improving the flow in this turn should increase the closed loop OHP's performance. [DOI: 10.1115/1.4003546]

Keywords: oscillating heat pipe, pulsating heat pipe, neutron radiography

1 Introduction

Electronic devices are being developed with ever increasing power density. The high heat fluxes require better cooling technologies to prevent overheating [1]. The oscillating heat pipe (OHP) is one of these devices that have a potential for high-heat-flux heat transfer [2]. An OHP consists of a capillary tube that crosses an evaporator and condenser multiple times. This tube is filled with a working fluid so that both liquid and vapor phases coexist. Due to the temperature difference between the evaporating and condensing sections, the saturation pressure in the evaporator is different from that in the condenser resulting in the driving force of the OHP. Combining with the vapor volume expansion in the evaporating section and contraction in the condensing section, these localized pressure changes create oscillating and circulating motions within the OHP transferring heat from the evaporator to the condenser via sensible and latent heat.

Fluid motion is the primary mechanism to transfer heat from the evaporator to the condenser within an OHP. The direct visualization is one of the most important aspects to better understand the oscillating motion effect on the heat transfer mechanism in an OHP. Visualizing an OHP is normally accomplished by using clear plastic or glass as a window into an OHP design [3–11]. While this method is useful, there are some aspects that are different than an all metal OHP. Glass and plastic have low thermal conductivities compared with metal; therefore, transient temperatures in the OHP are difficult to record. Also, each construction material has different surface properties such as surface tension and surface roughness, which can affect OHP performance. In this study, neutron radiography is utilized to collect video of fluid motion inside a copper OHP. This is possible because common heat pipe materials, such as copper and aluminum, are translucent to neutrons, while hydrogen rich fluids, such as water and acetone, are nearly opaque [8]. Four OHPs with the configurations of open loop water, open loop acetone, closed loop water, and closed loop acetone were investigated thermally and visually.

2 Experiment Setup and Procedure

Four OHPs were constructed for this experiment, two open loop (Fig. 1(*a*)) and two closed loop OHPs (Fig. 1(*b*)). Besides the tubing configuration, the two designs were identical. The overall size of the OHP was dictated by the camera size of the neutron imaging system. Therefore, a six turn OHP with overall dimensions of 15.5×15.5 cm^2 was chosen. The OHP tubing was sized to maintain capillary flow for water and acetone operating fluids. The OHPs were also designed to improve neutron transparency, by using materials appropriate for neutron radiography. The OHPs were constructed out of copper tubing and copper condenser and evaporator heat spreaders. These OHPs were constructed out of a 1.65 mm inner diameter and 3.18 mm outer diameter copper tube laid into 3.18 mm deep semicircular grooves machined into the 6.35 mm thick copper heat spreading plates. Semicircular grooves were used to improve contact between the plate and the round copper tubing. The evaporator plate was sized to match the strip heater's dimensions of 39×155 mm^2. A deuterium oxide, or heavy water, cooled aluminum block of 64×155 mm^2 was used to cool the copper condensing plate. The adiabatic region was 53 mm long. Omegatherm "201" thermal contact paste was used where necessary to reduce contact resistance. The heat pipes were charged with high performance liquid chromatography (HPLC) grade water or HPLC grade acetone at the filling ratios listed in Table 1. Each OHP was instrumented with 24 T-type calibrated thermocouples, as shown in Fig. 1. The maximum error of the calibrated thermocouples was ± 0.25°C. The resulting neutron image (Fig. 1(*d*)) clearly shows the dark liquid slugs and light vapor bubbles in the OHP.

Figure 2 shows the experimental setup. The OHP was placed inside a radiation shielded room, between the neutron source and the neutron imaging camera. Each OHP was encased in fiberglass and wrapped in aluminum foil to prevent airborne radioactive par-

[1]Corresponding author.

Contributed by the Heat Transfer Division of ASME for publication in the JOURNAL OF HEAT TRANSFER. Manuscript received June 2, 2010; final manuscript received December 16, 2010; published online March 8, 2011. Assoc. Editor: Louis C. Chow.

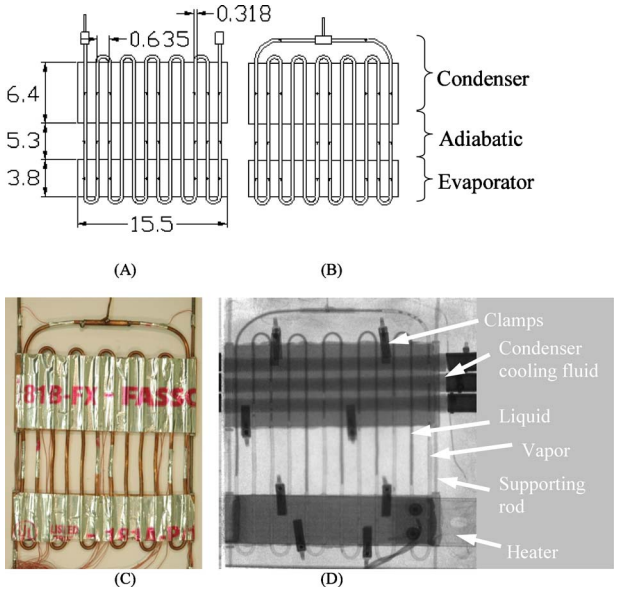

Fig. 1 OHP prototypes: (*a*) schematic of the open loop OHP, (*b*) schematic of the closed loop OHP, (*c*) photo of the finished OHP, and (*d*) neutron radiography image of the OHP (units in cm)

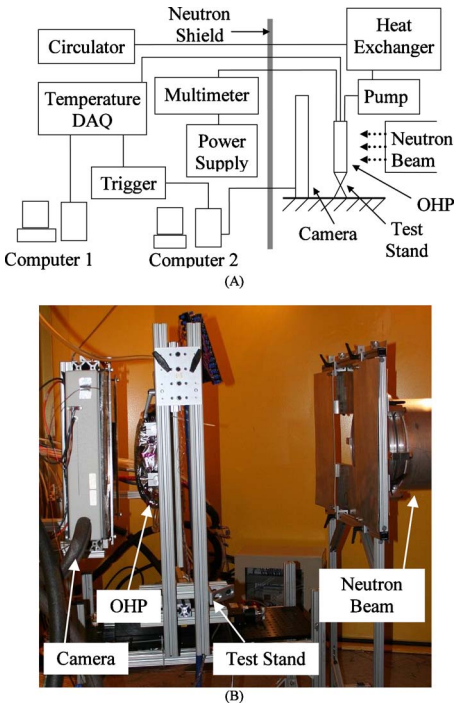

Fig. 2 Experimental setup: (*a*) schematic and (*b*) photo of neutron imaging system

ticulate. Because the OHPs were liquid cooled, a suitable fluid must be used that does not obstruct the OHP image. Heavy water was chosen for its high level of transparency compared with normal water. The heavy water loop was cooled via a heat exchanger by a Julabo F34 temperature controlled circulator. The circulator was filled with tap water. This heat exchanger loop allowed a minimal quantity of heavy water. The resulting temperature and visual data were collected simultaneously on separate computers. Temperature data were collected via a NI SCXI-1600 DAQ at 60 Hz and radiography images were collected at 30 frames/s.

3 Results and Discussion

Using the experimental setup shown in Fig. 2, experiments for four OHPs were conducted. Because both the thermal and visual data were obtained at the same time, the temperature and video can be directly compared with each other to better understand OHP operation. The effects of power, condenser temperature, working fluid, and orientation on the heat transfer performance were studied in these experiments. Because increasing power directly increases fluid velocity within the OHP, the resulting fluid motion in the neutron images at high fluid velocities caused the liquid/vapor interface to blur. Therefore, the power was increased until blurring became too significant, limiting the amount of useful information from the neutron images. For the acetone OHPs, this limit was 100 W and for the water OHPs, this limit was 300 W. Two condenser temperatures of 20°C and 60°C were used during this experiment. Also, two orientations were used, vertical with the condenser gravitationally above the evaporator and horizontal, where the OHP was rotated 90 deg in the vertical plane, resulting in the evaporator and condenser being side by side. The OHPs could only be tested in the vertical plane due to the neutron beam's orientation.

Figure 3 illustrates the temperature variations between the wa-

Table 1 Filling ratio of the OHPs

Heat pipe design	Fluid	Filling ratio
Open loop	Acetone	0.45
Open loop	Water	0.46
Closed loop	Acetone	0.48
Closed loop	Water	0.51

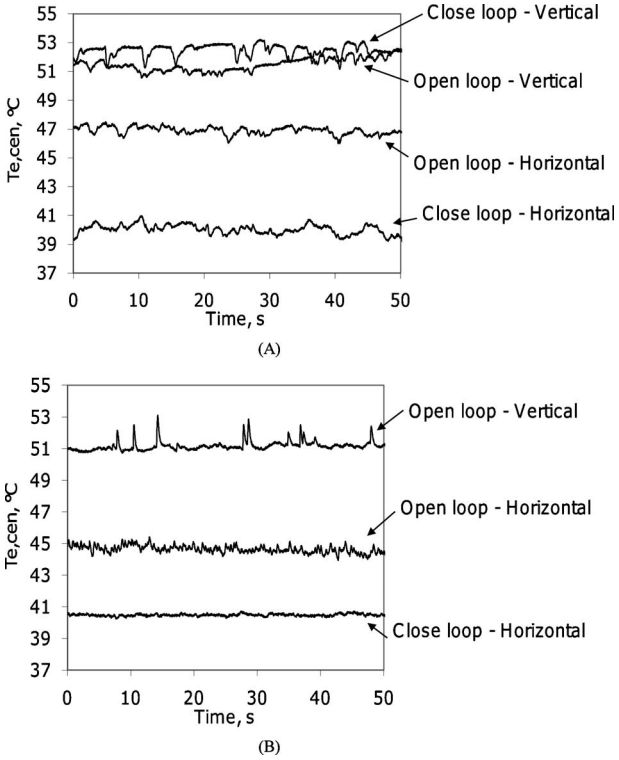

Fig. 3 Evaporator temperature oscillations at 100 W and a condenser temperature of 20°C: (*a*) water OHP and (*b*) acetone OHP

ter OHP and acetone OHP including the effects of orientation and loop type at a condenser temperature of 20°C and a power of 100 W. As shown in Fig. 3(*a*), the frequency and amplitude of the evaporator temperatures of the acetone OHP depend on orientation and loop type. The open loop vertical acetone OHP had the highest thermal amplitude and lowest frequency. The open loop horizontal acetone OHP had medium frequency and amplitude and the closed loop horizontal acetone OHP had the lowest amplitude but highest frequency. The closed loop vertical acetone OHP was not tested at 100 W due to the excessively high fluid velocity. The thermal amplitude for all water OHPs is greater than the acetone OHPs and the frequency of all water OHPs is less than acetone OHPs, as shown in Fig. 3(*b*).

However, visual data obtained by the neutron images show that the movement amplitude for all acetone OHPs is greater than all water OHPs at the same power input. While it is similar to those predicted by Ma et al. [12], it is very different from the thermal amplitude shown in Fig. 3. The thermal or temperature amplitude obtained herein is the temperature variation of the heat pipe wall surface. And the movement amplitude indicates the location variation of the mass center of the total liquid plugs and vapor bubbles in the OHP. Although the thermal amplitude is directly related to the movement amplitude, the thermal amplitude is very different from the movement amplitude, meaning that a higher movement amplitude may not result in a higher thermal amplitude. The thermal data are attenuated compared with the movement amplitude because of the thermal mass of the copper tubing. For example, if the time constant of the heat pipe wall is larger, the response time of the wall surface temperature is less than $1/f$, where f is the frequency of liquid plugs and vapor bubbles in the OHP, the thermal amplitude measured will be smaller than the movement amplitude of the liquid plugs and vapor bubbles in the OHP. It is concluded that the thermal amplitude cannot truly show the movement amplitude of liquid plugs and vapor bubbles in an OHP.

Due to the thermal mass of the copper tubing, there is a lag and attenuation in amplitude between the thermal and visual data. Figure 4 shows a direct comparison of the thermal and visual difference between the water and acetone OHPs at a condenser temperature of 60°C and an input power of 50 W. From the thermal data shown in Fig. 4(*a*), the frequency of evaporator temperature in the acetone OHP is much faster than that in the water OHP and the temperature amplitude is much smaller than the water OHP at a low power. The neutron visual images shown in Fig. 4(*b*) also demonstrate that the acetone OHP is oscillating much faster than the water OHP. The higher fluid frequency is visible as high velocity in the figure due to the blurring of the acetone liquid vapor interface, resulting in gray gradients. The water OHP has much slower flow, therefore a better defined liquid vapor interface. The acetone OHP always had higher frequency. It can be concluded that the acetone OHP can produce higher temperature uniformity in the evaporating section of an OHP at a low power compared with water OHPs.

Figures 5 illustrates the effects of power, condensing temperature, orientation, and working fluid type on the temperature difference between the evaporator and condenser in a closed loop oscillating heat pipe. As shown in Fig. 5, when the power increases, the temperature difference between the evaporator and condenser for both OHPs increases. However, the increase rate for the acetone OHP is very different from the water OHP. Figure 5 illustrates the general trends of tested OHPs. Vertical OHPs typically had a smaller temperature difference than horizontal OHPs. However, visually the flow patterns were similar. The thermal performance difference is due to gravity assisting in the OHP operation in the vertical orientation and only slightly assisting in the horizontal orientation. The similar visual flow pattern cannot readily be explained but likely there was a small difference in flow patterns that was not apparent. Another general trend was that higher condenser temperatures always had lower temperature difference, and visually the only difference was increased fluid velocity. The reduced thermal resistance with increased condenser temperature is due to the superior fluid properties at high temperatures. These improved properties include increased $(\partial P/\partial T)_{\text{sat}}$ and reduced viscosity. Comparing the acetone and water OHPs, as shown in Fig. 5, the acetone OHP has a smaller temperature difference at low power input compared with the water OHP. At 25 W, the closed loop acetone OHP in the vertical orientation and the condenser at 20°C had an average temperature difference of 2.3°C, whereas the closed loop water OHP had an average temperature difference of 4.3°C. This is primarily due to the higher frequency of the acetone OHP. However, at higher heat fluxes, the water OHP frequency increases and water's superior fluid properties prevail causing the water OHP having a smaller average temperature difference than acetone.

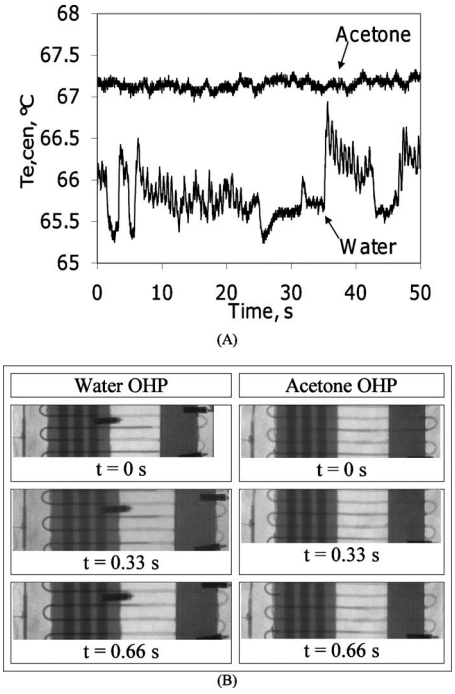

Fig. 4 A comparison of thermal data with neutron images of the closed loop water and acetone OHPs in the horizontal orientation at 50 W and a condenser temperature of 60°C: (*a*) evaporator temperature and (*b*) neutron images of fluid movement

Figure 6 illustrates the flow patterns in both the closed and open loop OHPs providing a view of the oscillating motion. Figure 6 was made by calculating the standard deviation of each pixel with time for an entire 2 min video. In the video, when the interface of the fluid passed across a pixel, the pixel changed from dark to light. This change in intensity results in a high standard deviation. In the middle of a liquid slug or vapor bubble, the pixels are always the same intensity and therefore have a low standard deviation. In Fig. 6, the regions with high standard deviations are light colored and regions with low standard deviations are dark. From results shown in Fig. 6, it can be seen that closed loop OHPs have much greater liquid movement throughout compared with open loop OHPs. The open loop OHPs experience only localized motion of interfaces and this is minimal in the outer turns. The reduced flow lowers the heat transport capability of the open loop design. In the open loop designs, the water OHP has more movement than the acetone OHP. The advantage of the closed loop OHP design is that the outer turns are connected, allowing fluid and pressure to transfer between the two sides and throughout the entire OHP. However, it was visually observed that the water closed loop OHP never fully circulates. Therefore, pressure was transferring between the two sides, but not fluid. In effect, the

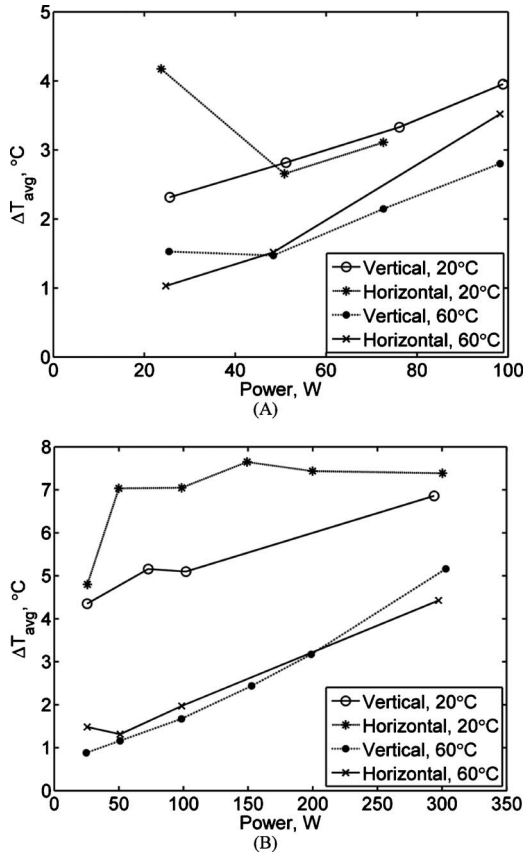

Fig. 5 The average temperature difference of (*a*) the closed loop acetone oscillating heat pipe and (*b*) closed loop water oscillating heat pipe at condenser temperatures of 20°C and 60°C and in a vertical and horizontal orientation

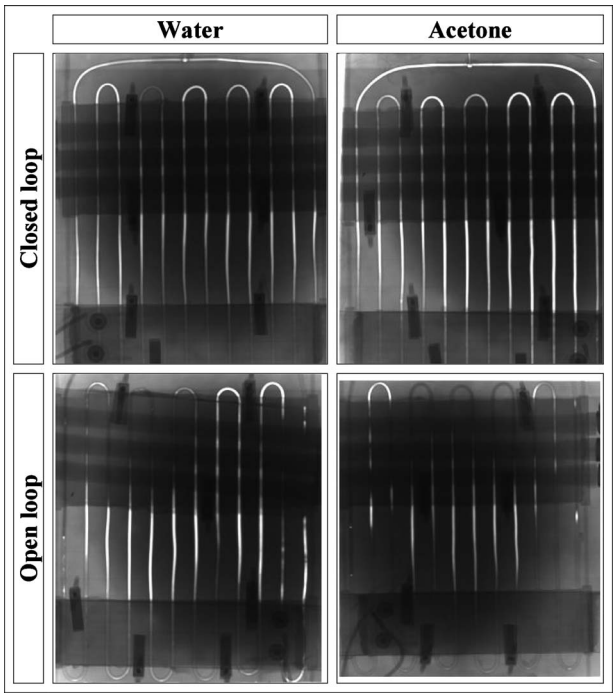

Fig. 6 The pixel standard deviation for the open and closed loops, water, and acetone OHPs (vertical orientation with a power input of 50 W and a condenser temperature of 60°C). The bright regions are where the standard deviation is highest.

operation of the closed loop water OHP is very similar to the open loop water OHP. Thermally, these two OHPs also perform very similarly. The acetone OHP was found to fully circulate but only at high heat flux. However, the acetone OHP at high heat flux, the fluid slows down in the turn connecting the two sides but does move into other turns eventually. For acetone, full circulation was achieved and the thermal performance was much better for the closed loop design. Therefore, full circulation of fluid is very important to the thermal performance of the OHP. These results were independent of orientation and condenser temperature.

4 Conclusions

Four OHPs were compared using neutron radiography and thermocouples. Increased condenser temperature was shown to significantly increase OHP performance. However, visually, the only flow difference is the increased velocity. Orientation had little effect on OHP performance at high condenser temperatures. At low condenser temperatures, vertical orientation performed better than horizontal. This is primarily due to the unfavorable change in fluid properties at lower temperatures, mainly the reduction in $(\partial P/\partial T)_{sat}$. The acetone OHP was shown to have higher fluid velocities and better fluid circulation, where the water OHP did not have circulation and the fluid movement was sporadic. At high powers, the water OHP movement became much more frequent and its heat transport capability greatly increased. Both the acetone and water closed loop OHPs had reduced fluid movement in the turn connecting the two sides. In the closed loop water OHP, it prevented circulation. This is due to the long distance of the turn without any heating or cooling, which directly affects the local pressure variation. The optimal OHP for low power was the vertical closed loop acetone OHP and at high power the vertical closed loop water OHP. Reducing the length of the turn connecting the two sides could further improve these OHPs.

Acknowledgment

The work presented in this article was funded by the Office of Naval Research, Grant No. N00014-06-1-1119 directed by Dr. Mark Spector and National Institute of Standards and Technology.

Nomenclature

T = temperature, °C
ΔT = temperature difference, °C

Subscripts

avg = average
cen = center
e = evaporator
sat = saturation

References

[1] Chu, R. C., Simons, R. E., Ellsworth, M. J., Schmidt, R. R., and Cozzolino, V., 2004, "Review of Cooling Technologies for Computer Products," IEEE Trans. Device Mater. Reliab., **4**(4), pp. 568–585.
[2] Zhang, Y., and Faghri, A., 2008, "Advances and Unsolved Issues in Pulsating Heat Pipes," Heat Transfer Eng., **29**, pp. 20–44.
[3] Charoensawan, P., Khandekar, S., Groll, M., and Terdtoon, P., 2003, "Closed Loop Pulsating Heat Pipes Part A: Parametric Experimental Investigations," Appl. Therm. Eng., **23**, pp. 2009–2020.
[4] Xu, J. L., Li, Y. X., and Wong, T. N., 2005, "High Speed Flow Visualization of a Closed Loop Pulsating Heat Pipe," Heat Mass Transfer, **48**, pp. 3338–3351.
[5] Khandekar, S., Schneider, M., Schafer, P., Kulenovic, R., and Groll, M., 2002, "Thermofluid Dynamic Study of Flat-Plate Closed-Loop Pulsating Heat Pipes," Microscale Thermophys. Eng., **6**, pp. 303–317.
[6] Cai, Q., Chen, R., and Chen, C., 2002, "An Investigation of Evaporation, Boiling, and Heat Transport Performance in Pulsating Heat Pipe," *Proceedings of IMECE2002 ASME International Mechanical Engineering Congress & Exposition*, pp. 99–104.
[7] Khandekar, S., and Groll, M., 2004, "An Insight Into Thermo-Hydrodynamic Coupling in Closed Loop Pulsating Heat Pipes," Int. J. Therm. Sci., **43**, pp. 13–20.

[8] Wilson, C., Borgmeyer, B., Winholtz, R., Ma, H., Jacobson, D., Hussey, D., and Arif, M., 2008, "Visual Observation of Oscillating Heat Pipes Using Neutron Radiography," J. Thermophys. Heat Transfer, **22**, pp. 366–372.
[9] Qu, J., and Wu, H.,2010, "Flow Visualization of Silicon-Based Micro Pulsating Heat Pipes," Science China Technological Science, **53**(4), pp. 984–990.
[10] Yuan, D., Qu, W., and Ma, T., 2010, "Flow and Heat Transfer of Liquid Plug and Neighboring Vapor Slugs in a Pulsating Heat Pipe," Int. J. Heat Mass Transfer, **53**(7–8), pp. 1260–1268.
[11] Ma, H. B., Hanlon, M. A., and Chen, C. L., 2006, "An Investigation of Oscillating Motions in a Miniature Pulsating Heat Pipe," Microfluid. Nanofluid., **2**, pp. 171–179.
[12] Ma, H. B., Borgmeyer, B., Cheng, P., and Zhang, Y., 2008, "Heat Transport Capability in an Oscillating Heat Pipe," ASME J. Heat Transfer, **130**, p. 081501.